

Diffraction and the Reciprocal Lattice

DIFFRACTION

In this chapter, *diffraction*, the scattering of a coherent wave by a crystal, is considered. Given the wave-particle duality of nature, the elastic scattering of a beam of particles from a crystal is also discussed. The projectile particles may be x-rays, neutrons, or high-energy electrons. These particles are able to penetrate the bulk of the material and provide information concerning its three-dimensional geometric and chemical structure. Other scattering probes, such as low-energy electrons or atomic beams, are not as penetrating and are more useful for studying the surface region of a solid. Diffraction is sensitive to the translational periodicity presented by the crystal. For a periodic solid, scattering occurs only into a discrete set of directions in space. The strength of the scattering is determined by the nature of both the probe and the target. In the case of x-ray scattering it is the electron density that determines the scattering amplitude. For neutrons it is the nuclear force that is responsible. In both cases the lattice potential determining the dynamics has translational periodicity.

For diffraction patterns to be observable, the characteristic wavelengths of the probe beam must be on the order of or smaller than (twice the) interatomic spacings in the solid. For example, a 10-keV x-ray has a wavelength $\lambda = 0.124$ nm, a thermal neutron (with kinetic energy 1/40 eV) has a de Broglie wavelength $\lambda = 0.181$ nm, and a 100-keV electron has $\lambda = 0.0037$ nm. The wavelength of the x-ray in terms of its energy E is given by $\lambda = hc/E$. For the neutron it is given by $\lambda = h/\sqrt{2m_n T}$, where T is its kinetic energy. For the electron it is given by the relativistic formula $\lambda = h/\sqrt{T(2m_e + T/c^2)}$. Here h is Planck's constant, c is the speed of light, and m_n and m_e are the rest masses of the neutron and electron, respectively.

X-rays were discovered in 1895 by W. Roentgen when he analyzed the emanations produced by the impact of high-energy cathode rays (electrons) on metallic anodes. Evidence for the electromagnetic nature of this radiation was provided in 1912 by W. Friedrich, P. Knipping, and M. von Laue when they passed a beam of x-rays through a crystal and observed a pattern of diffraction spots. These were analogous to the diffraction pattern observed when visible light passed through a pair of crossed diffraction gratings. A systematic study of diffraction spots produced during x-ray reflection allowed W. H. Bragg and W. L. Bragg in 1913 to extract detailed structural and symmetry information for a broad range of crystals. The use of x-ray diffraction techniques has continued to this day. Synchrotron radiation sources provide scientists and engineers with a tunable source of x-ray wavelengths. Large biomolecules may be crystallized and their structures may be determined using x-ray diffraction methods. X-ray diffraction has become the tool of choice for studying the structure of all types

of materials. Although most effective for crystalline materials, where a full characterization is often possible, diffraction also provides useful information about disordered materials. X-rays are discussed further at our Web site in Chapter W22.[†]

This chapter begins with a discussion of Fourier analysis in one and three dimensions and introduces the reciprocal lattice. We then proceed to discuss elastic scattering from both ordered and disordered materials. The latter include polycrystalline and amorphous solids. An analysis of how the internal structure of the unit cell may be determined is given at our Web site.

3.1 Fourier Analysis in One and Three Dimensions

The incident beam is taken to be monochromatic (or monoenergetic) and well collimated (unidirectional). It is represented by a plane wave $\psi = \exp[i(\mathbf{k} \cdot \mathbf{r} - \omega t)]$ with wave vector \mathbf{k} and angular frequency ω . In describing diffraction one must know how this wave scatters into another wave ψ' with wave vector \mathbf{k}' but with the same frequency ω . The scattering amplitude is determined by an integral of the form $\int d\mathbf{r} \psi'^* V \psi$, where V describes some physical property of the crystal which depends on the nature of the probe. Whatever this quantity is, be it electron density for x-ray scattering, the nuclear potential for neutron scattering, or the lattice potential for electron scattering, the quantity V will often, but not always, be a periodic function of space. In this section it will be seen how Fourier analysis allows one to express mathematically what is happening in x-ray diffraction.

A periodic function in one dimension such that

$$V(x) = V(x \pm a) \quad (3.1)$$

may be represented as a Fourier series:

$$V(x) = \sum_{n=-\infty}^{\infty} V_n e^{i(2\pi n x/a)}, \quad (3.2)$$

where the Fourier coefficients V_n may be found by multiplying through by $\exp[-i(2\pi m x/a)]$ and integrating over the spatial period. Use is made of the integral

$$\int_0^a e^{i[2\pi(n-m)x/a]} dx = a \delta_{m,n} \quad (3.3)$$

where $\delta_{m,n}$, called *Kronecker's delta*, is 1 if $m = n$ and 0 otherwise. The formula for the Fourier coefficients is

$$V_n = \frac{1}{a} \int_0^a V(x) e^{-i(2\pi n x/a)} dx. \quad (3.4)$$

In a similar way a three-dimensional periodic function $V(\mathbf{r})$ may be invariant under translation by a Bravais lattice vector \mathbf{R} :

$$V(\mathbf{r} + \mathbf{R}) = V(\mathbf{r}). \quad (3.5)$$

[†] Supplementary material for this textbook is included on the Web at the resource site (ftp://ftp.wiley.com/public/sci_tech_med/materials). Cross-references to elements of the Web material are prefixed by "W."

The problem is to generalize the foregoing Fourier analysis technique to three dimensions. To this end, \mathbf{R} is expressed as a linear combination of primitive lattice translation vectors,

$$\mathbf{R} = n_1 \mathbf{u}_1 + n_2 \mathbf{u}_2 + n_3 \mathbf{u}_3, \quad (3.6)$$

where $\{n_1, n_2, n_3\}$ are a set of integers. Introduce a set of primitive reciprocal lattice vectors $\{\mathbf{g}_1, \mathbf{g}_2, \mathbf{g}_3\}$ such that

$$\mathbf{g}_i \cdot \mathbf{u}_j = 2\pi \delta_{i,j}, \quad i = 1, 2, 3, \quad j = 1, 2, 3. \quad (3.7)$$

Explicit formulas for the \mathbf{g}_i are given by the expressions

$$\mathbf{g}_1 = 2\pi \frac{\mathbf{u}_2 \times \mathbf{u}_3}{\mathbf{u}_1 \cdot \mathbf{u}_2 \times \mathbf{u}_3}, \quad \mathbf{g}_2 = 2\pi \frac{\mathbf{u}_3 \times \mathbf{u}_1}{\mathbf{u}_1 \cdot \mathbf{u}_2 \times \mathbf{u}_3}, \quad \mathbf{g}_3 = 2\pi \frac{\mathbf{u}_1 \times \mathbf{u}_2}{\mathbf{u}_1 \cdot \mathbf{u}_2 \times \mathbf{u}_3}. \quad (3.8)$$

A general reciprocal lattice vector is expressed as a linear combination of the primitive reciprocal lattice vectors with integer coefficients

$$\mathbf{G} = j_1 \mathbf{g}_1 + j_2 \mathbf{g}_2 + j_3 \mathbf{g}_3 \quad (3.9)$$

and is thus described by a set of three integers $\{j_1, j_2, j_3\}$. The concept of the reciprocal lattice will play an important role in the understanding of the electron band structure of crystals, as described in Chapter 7.

The Fourier expansion of the crystal potential is

$$V(\mathbf{r}) = \sum_{\mathbf{G}} V_{\mathbf{G}} e^{i\mathbf{G} \cdot \mathbf{r}}, \quad (3.10)$$

where $\{V_{\mathbf{G}}\}$ are a set of Fourier coefficients. Periodicity is obvious since

$$\begin{aligned} V(\mathbf{r} + \mathbf{R}) &= \sum_{\mathbf{G}} V_{\mathbf{G}} e^{i\mathbf{G} \cdot (\mathbf{r} + \mathbf{R})} = \sum_{\mathbf{G}} V_{\mathbf{G}} e^{i\mathbf{G} \cdot \mathbf{r}} e^{i2\pi(j_1 n_1 + j_2 n_2 + j_3 n_3)} \\ &= \sum_{\mathbf{G}} V_{\mathbf{G}} e^{i\mathbf{G} \cdot \mathbf{r}} = V(\mathbf{r}). \end{aligned} \quad (3.11)$$

In the one-dimensional case the basic unit cell is the interval $0 < x < a$. The analogous volume unit in the three-dimensional case is called the *Wigner-Seitz cell*, defined as follows. Select any point in the crystal as a reference point and label it O . Replicate that point by translating it through all possible lattice translation vectors \mathbf{R} and label the resulting set $\{O_{\mathbf{R}}\}$. The Wigner-Seitz (WS) cell is the set of all points \mathbf{r} in the crystal that are closer to O than to any other $O_{\mathbf{R}}$. The boundary of the WS cell has a polyhedral shape. Every point on a face of the polyhedron has a corresponding point on an opposite face that may be reached by a primitive lattice translation vector.

An alternative way of constructing the WS cell is to single out a particular atom, S , and to draw lines to all other atoms occupying the same basis site in other lattice cells. Introduce the perpendicular bisecting planes of these lines. Atom S will then be surrounded by a polyhedral shape. This is also a WS cell.

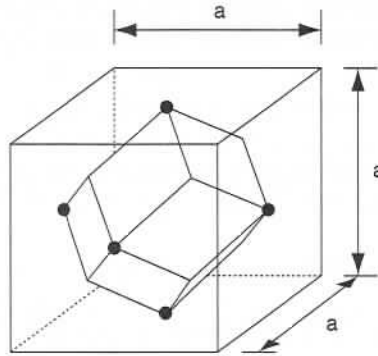


Figure 3.1. Wigner–Seitz cell for the FCC lattice. The heavy dots are at the centers of the faces of the cube.

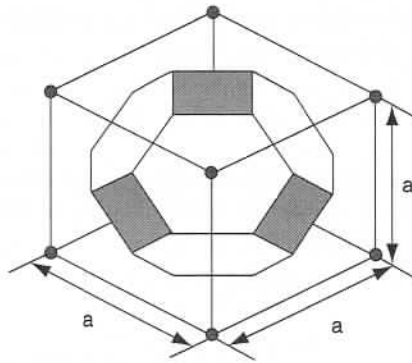


Figure 3.2. Wigner–Seitz cell for the BCC lattice. The shaded squares are on the surface of the cube.

Figure 3.1 illustrates the WS cell for the FCC lattice. It is a regular rhombic dodecahedron whose bounding surface consists of 12 squares perpendicular to the $\langle 110 \rangle$ directions. The WS cell for the BCC lattice is the truncated octahedron given in Fig. 3.2. Its bounding surface consists of six squares oriented perpendicular to the $\langle 100 \rangle$ directions and eight regular hexagons perpendicular to the $\langle 111 \rangle$ directions.

The following orthogonality identity holds:

$$\int_{\text{WS}} e^{i(\mathbf{G}-\mathbf{G}')\cdot\mathbf{r}} d\mathbf{r} = V_{\text{WS}} \delta_{\mathbf{G},\mathbf{G}'}, \quad (3.12)$$

where the integral $d\mathbf{r}$ is over the volume of the Wigner–Seitz cell. This gives a formula for the Fourier coefficients:

$$V_{\mathbf{G}} = \frac{1}{V_{\text{WS}}} \int_{\text{WS}} V(\mathbf{r}) e^{-i\mathbf{G}\cdot\mathbf{r}} d\mathbf{r}. \quad (3.13)$$

An explicit formula for the volume of the Wigner–Seitz cell is

$$V_{\text{WS}} = |\mathbf{u}_1 \cdot \mathbf{u}_2 \times \mathbf{u}_3|. \quad (3.14)$$

Note that the volume of the WS cell is the same as that of the primitive unit cell defined in Chapter 1.

In the expression for \mathbf{G} in Eq. (3.9), three integers were introduced, $\{j_1, j_2, j_3\}$. If these integers have a common integer divisor, \mathbf{G} will be called *reducible*. If there is no common integer divisor, \mathbf{G} is *irreducible*. Thus the set $\{2,4,6\}$ is reducible, whereas $\{1,2,3\}$ is irreducible.

The reciprocal lattice vectors may be given a simple geometric interpretation. Select an origin O in real space and look at the set of points described by vectors \mathbf{r} originating at O and satisfying the equation

$$\mathbf{G} \cdot \mathbf{r} = 2\pi \rightarrow \hat{G} \cdot \mathbf{r} = \frac{2\pi}{G}, \quad (3.15)$$

where \hat{G} is a unit vector and \mathbf{G} is irreducible. A linear equation of the form $G_x X + G_y Y + G_z Z = 2\pi$ defines a plane in the direct lattice. This plane lies a distance $d = 2\pi/G$ from O and its normal is oriented along \mathbf{G} . There are, in fact, an infinite set of parallel planes described by the equations

$$\mathbf{G} \cdot \mathbf{r} = 2\pi N \rightarrow \hat{G} \cdot \mathbf{r} = \frac{2\pi N}{G}, \quad (3.16)$$

where N is any integer and \mathbf{G} is reducible. The spacing between successive planes is $d = 2\pi/G$, where \mathbf{G} is irreducible. The significance of these lattice planes will be seen shortly.

Suppose that \mathbf{G} is irreducible and look at the intersection of the plane defined by $\mathbf{G} \cdot \mathbf{r} = 2\pi$ with the axes defined by the vectors $\{\mathbf{u}_1, \mathbf{u}_2, \mathbf{u}_3\}$. For $\mathbf{r} = \mathbf{u}_1/h$, one obtains $\mathbf{G} \cdot \mathbf{r} = 2\pi j_1/h = 2\pi$, so $j_1 = h$. Similarly, if one writes $\mathbf{r} = \mathbf{u}_2/k$, one obtains $\mathbf{G} \cdot \mathbf{r} = 2\pi j_2/k = 2\pi$, so $j_2 = k$. Finally, for $\mathbf{r} = \mathbf{u}_3/l$, one finds $j_3 = l$. Thus the components of the \mathbf{G} vector expressed in terms of the primitive reciprocal lattice vectors can be given a simple geometrical interpretation. The intersection of the lattice planes with the primitive axes occurs at coordinates that are inversely proportional to the coefficients j_1, j_2 , and j_3 . The coefficients (hkl) are referred to as the *Miller indices* of the plane, as discussed in Section 1.5.

3.2 Examples of Reciprocal Lattices

Reciprocal lattices corresponding to the various Bravais lattices are simple to generate. Starting with the class of cubic crystals, the primitive translation vectors for the simple cubic (SC) lattice may be chosen as

$$\mathbf{u}_1 = a\hat{i}, \quad \mathbf{u}_2 = a\hat{j}, \quad \mathbf{u}_3 = a\hat{k}. \quad (3.17)$$

The volume of the unit cell is a^3 and the primitive reciprocal lattice vectors, determined from Eq. (3.8), are

$$\mathbf{g}_1 = \frac{2\pi}{a}\hat{i}, \quad \mathbf{g}_2 = \frac{2\pi}{a}\hat{j}, \quad \mathbf{g}_3 = \frac{2\pi}{a}\hat{k}. \quad (3.18)$$

The orthogonality relations of Eq. (3.7) are obvious.

For the FCC lattice the primitive translation vectors may be chosen in the symmetric form

$$\mathbf{u}_1 = \frac{a}{2}(\hat{j} + \hat{k}), \quad \mathbf{u}_2 = \frac{a}{2}(\hat{k} + \hat{i}), \quad \mathbf{u}_3 = \frac{a}{2}(\hat{i} + \hat{j}), \quad (3.19)$$

as shown in Fig. 1.5. The volume of the unit cell is $a^3/4$. The primitive reciprocal lattice vectors are

$$\mathbf{g}_1 = \frac{2\pi}{a}(-\hat{i} + \hat{j} + \hat{k}), \quad \mathbf{g}_2 = \frac{2\pi}{a}(\hat{i} - \hat{j} + \hat{k}), \quad \mathbf{g}_3 = \frac{2\pi}{a}(\hat{i} + \hat{j} - \hat{k}). \quad (3.20)$$

For the BCC lattice the corresponding vectors are

$$\mathbf{u}_1 = \frac{a}{2}(-\hat{i} + \hat{j} + \hat{k}), \quad \mathbf{u}_2 = \frac{a}{2}(\hat{i} - \hat{j} + \hat{k}), \quad \mathbf{u}_3 = \frac{a}{2}(\hat{i} + \hat{j} - \hat{k}), \quad (3.21)$$

as shown in Fig. 1.4. The volume of the unit cell is $a^3/2$ and

$$\mathbf{g}_1 = \frac{2\pi}{a}(\hat{j} + \hat{k}), \quad \mathbf{g}_2 = \frac{2\pi}{a}(\hat{i} + \hat{k}), \quad \mathbf{g}_3 = \frac{2\pi}{a}(\hat{i} + \hat{j}). \quad (3.22)$$

Note that the BCC lattice of lattice constant a in real space generates an FCC lattice of lattice constant $4\pi/a$ in reciprocal space, whereas the FCC lattice of lattice constant a in real space produces a BCC lattice of lattice constant $4\pi/a$ in reciprocal space. For the SC lattice the reciprocal is also SC, but with lattice constant $2\pi/a$. The relation

$$e^{i\mathbf{G}\cdot\mathbf{R}} = 1 \quad (3.23)$$

is the formula connecting the two lattices, so it is clear that if the $\{\mathbf{R}\}$ vectors form a Bravais lattice, so should the $\{\mathbf{G}\}$ vectors. From the symmetry between \mathbf{G} and \mathbf{R} in this formula, it follows that the reciprocal of the reciprocal lattice is again the direct lattice in real space.

Also note that just as the primitive translation vectors are not unique, neither are the primitive reciprocal lattice vectors. For example, return to the SC lattice and choose

$$\mathbf{u}_1 = a\hat{i}, \quad \mathbf{u}_2 = a\hat{j}, \quad \mathbf{u}_3 = a(\hat{i} + \hat{j} + \hat{k}). \quad (3.24)$$

The volume of the unit cell is still a^3 and the reciprocal lattice vectors are

$$\mathbf{g}_1 = \frac{2\pi}{a}(\hat{i} - \hat{k}), \quad \mathbf{g}_2 = \frac{2\pi}{a}\hat{j}, \quad \mathbf{g}_3 = \frac{2\pi}{a}\hat{k}. \quad (3.25)$$

This is an acceptable set of lattice vectors but is not desirable because it does not conform to the underlying symmetry of the crystal.

The structure in reciprocal space which is analogous to the Wigner-Seitz cell in real space is the first Brillouin zone (FBZ). One imagines a lattice of reciprocal lattice points (defined by $\{\mathbf{G}\}$) in wave vector space (\mathbf{k} space) with the origin chosen as \mathbf{O} . All points in \mathbf{k} space closer to \mathbf{O} than to any other \mathbf{G} are in the FBZ. Like the WS cell, the FBZ, has a polyhedral shape. The volume of the FBZ Ω is

$$\begin{aligned} \Omega &= |\mathbf{g}_1 \cdot \mathbf{g}_2 \times \mathbf{g}_3| = \frac{(2\pi)^3}{|\mathbf{u}_1 \cdot \mathbf{u}_2 \times \mathbf{u}_3|^3} |(\mathbf{u}_2 \times \mathbf{u}_3) \cdot (\mathbf{u}_3 \times \mathbf{u}_1) \times (\mathbf{u}_1 \times \mathbf{u}_2)| \\ &= \frac{(2\pi)^3}{|\mathbf{u}_1 \cdot \mathbf{u}_2 \times \mathbf{u}_3|} = \frac{(2\pi)^3}{V_{\text{WS}}}. \end{aligned} \quad (3.26)$$

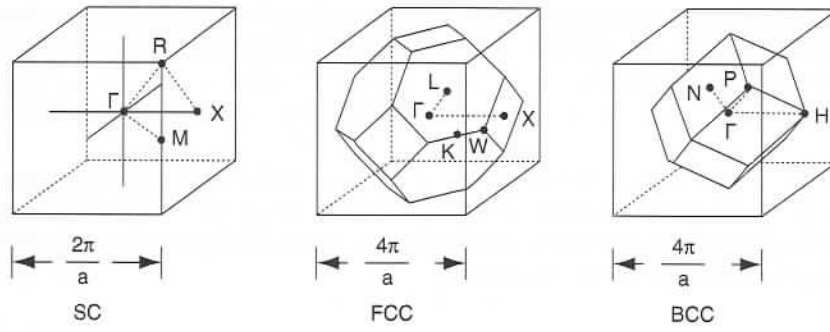


Figure 3.3. First Brillouin zones for the simple cubic, face-centered cubic, and body-centered cubic lattices.

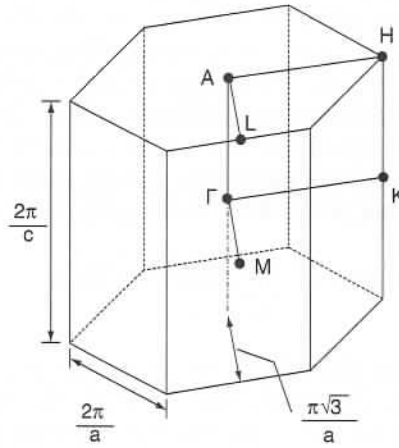


Figure 3.4. First Brillouin zone for the hexagonal lattice.

In Fig. 3.3 the FBZs for the SC, FCC, and BCC lattices are presented. In Fig. 3.4 the FBZ for the hexagonal lattice is sketched. The center of the zone is always called the Γ -point and corresponds to $\mathbf{k} = 0$. Other special points in the Brillouin zone are denoted by various alphabetical characters, as shown.

ELASTIC SCATTERING FROM ORDERED AND DISORDERED MATERIALS

In a scattering process there is momentum transfer and energy transfer between the projectile and the solid. An incoming particle with momentum \mathbf{p} is scattered to a state with momentum \mathbf{p}' with the momentum transfer

$$\mathbf{p}' - \mathbf{p} = \hbar\mathbf{q}. \tag{3.27}$$

Similarly, the projectile's energy E is changed to E' with the energy transfer

$$E' - E = \hbar\omega. \tag{3.28}$$

In this chapter attention is restricted to the case of elastic scattering, so that $E' = E$.

For x-rays the energy and momentum are related by $E = pc$. Energy conservation then implies that the magnitude of the momentum is conserved; that is,

$$p' = p. \quad (3.29)$$

For electrons and neutrons the nonrelativistic formula relating energy and momentum is $E = p^2/2m$, with m being the appropriate mass. Energy conservation again implies that $p' = p$. (This remains true even relativistically.) If ϕ denotes the angle between vectors \mathbf{p}' and \mathbf{p} , it is readily shown that

$$q = 2\frac{p}{\hbar} \sin \frac{\phi}{2}. \quad (3.30)$$

The scattering geometry is illustrated in Fig. 3.5.

In many situations the amplitude for the wave scattered from a collection of atoms may be expressed as the superposition of scatterings from the individual atoms. Later in the discussion of x-ray scattering (see Chapter W22) it will be seen that the scattering is from electrons, and these are usually associated with given atomic sites. In the case of neutron scattering it is the nuclei that act as scattering centers. For high-energy electrons the scattering is due largely to ion-electron interaction. In these three cases the scattering amplitude may be expressed as a superposition of contributions from the atomic sites $\{\mathbf{A}\}$:

$$F(\mathbf{q}) = \sum_{\mathbf{A}} f_{\mathbf{A}}(\mathbf{q}) \exp(i\mathbf{q} \cdot \mathbf{A}), \quad (3.31)$$

where $f_{\mathbf{A}}(\mathbf{q})$ is the atomic form factor for a given atom and \mathbf{q} is the wave vector transfer for the projectile. The sum extends over all the atoms in the crystal. The scattering intensity is proportional to the absolute square of the amplitude:

$$I(q) \propto I_0 |F(\mathbf{q})|^2, \quad (3.32)$$

where I_0 is the incident flux. The quantity $I(q)$ is what is measured in a diffraction or scattering experiment. Note that the phase information contained in F is lost in taking this absolute square.

In the analysis above the role of spin or polarization of the probe particles has been neglected. This is an approximation, although usually a good one. Notable exceptions occur, for example, when one uses polarized x-rays or scatters neutrons from

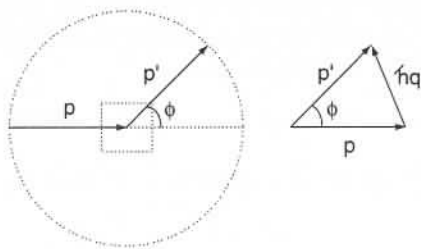


Figure 3.5. Scattering geometry.

magnetic materials. In such cases the spin degrees of freedom must be accounted for, and additional amplitudes need to be introduced. Detailed information concerning the alignment of the nuclear spins in the solid may be obtained from such experiments. Characterization of materials using x-rays is discussed in Chapter W22.

3.3 Crystalline Solids

Consider a crystal defined by a Bravais lattice and a set of basis atoms. The positions of the atoms are

$$\mathbf{A}_j(\mathbf{R}) = \mathbf{R} + \mathbf{s}_j, \quad (3.33)$$

where $\{\mathbf{R}\}$ is a set of Bravais lattice vectors, each pointing to a particular unit cell, and $\{\mathbf{s}_j\}$ is a set of basis vectors locating the atoms within the unit cell. In place of the single subscript \mathbf{A} used before, there are now dual indices, $(\mathbf{R}, \mathbf{s}_j)$. The scattering amplitude is expressed as

$$F(\mathbf{q}) = \sum_{\mathbf{R}} \sum_j f_j(\mathbf{q}) e^{i\mathbf{q} \cdot (\mathbf{R} + \mathbf{s}_j)} = \Phi(\mathbf{q})L, \quad (3.34)$$

where $\Phi(\mathbf{q})$ is the *structure factor* of the basis, defined by

$$\Phi(\mathbf{q}) = \sum_j f_j(\mathbf{q}) e^{i\mathbf{q} \cdot \mathbf{s}_j}, \quad (3.35)$$

and L is the lattice sum,

$$L = \sum_{\mathbf{R}} e^{i\mathbf{q} \cdot \mathbf{R}}. \quad (3.36)$$

In the expression for L , all lattice sites are included. If \mathbf{R} were to be replaced by $\mathbf{R} + \mathbf{R}'$, all lattice sites would still be included and the value of L should not change. Therefore,

$$\sum_{\mathbf{R}} e^{i\mathbf{q} \cdot \mathbf{R}} = \sum_{\mathbf{R}} e^{i\mathbf{q} \cdot (\mathbf{R} + \mathbf{R}')}, \quad (3.37)$$

or

$$(1 - e^{i\mathbf{q} \cdot \mathbf{R}'}) L = 0. \quad (3.38)$$

Either $\exp(i\mathbf{q} \cdot \mathbf{R}') = 1$, in which case \mathbf{q} is any reciprocal lattice vector or else L vanishes. Thus the scattering amplitude reduces to

$$F(\mathbf{q}) = N\Phi(\mathbf{q}) \sum_{\mathbf{G}} \delta_{\mathbf{q},\mathbf{G}}, \quad (3.39)$$

where N is the number of unit cells in the crystal. The scattering intensity becomes

$$I \sim I_0 N^2 \sum_{\mathbf{G}} \delta_{\mathbf{q},\mathbf{G}} |\Phi(\mathbf{q})|^2 = I_0 N^2 \sum_{\mathbf{G}} \delta_{\mathbf{q},\mathbf{G}} |\Phi(\mathbf{G})|^2. \quad (3.40)$$

The spectrum consists of a set of discrete points in \mathbf{q} space. The directions of the \mathbf{G} vectors determine the allowed momentum transfers and hence the directions of the diffracted peaks in real space.

The atomic form factors for x-ray scattering are proportional to the Fourier transforms of the electron density $n(\mathbf{r})$:

$$f(\mathbf{q}) \propto \int n(\mathbf{r})e^{-i\mathbf{q}\cdot\mathbf{r}} d\mathbf{r}. \quad (3.41)$$

When only a single atom is present, the integral extends over all space. For forward scattering, this is just proportional to the number of electrons, Z :

$$f(\mathbf{0}) \propto \int n(\mathbf{r}) d\mathbf{r} = Z. \quad (3.42)$$

Thus materials with large atomic numbers will scatter x-rays more efficiently than materials with low Z . With increasing q the form factor tends to fall off. For example, suppose that there is an exponential model for the falloff of n with distance from an isolated atom:

$$n(\mathbf{r}) = \frac{Z}{\pi a^3} e^{-2r/a}, \quad (3.43)$$

where a is on the order of the size of the atom. The corresponding atomic form factor is

$$f(\mathbf{q}) \sim \frac{Z}{1 + (qa/2)^2}, \quad (3.44)$$

which shows the rapid decline of $f(\mathbf{q})$ with q when $qa \gg 1$.

Note that for a monatomic crystal

$$\Phi(\mathbf{G}) = f(\mathbf{G})S(\mathbf{G}), \quad (3.45)$$

where

$$S(\mathbf{G}) = \sum_j e^{i\mathbf{G}\cdot\mathbf{s}_j} \quad (3.46)$$

is called the *geometric structure factor*. If there is only one atom per unit cell, such as in a primitive BCC or FCC lattice, $S(\mathbf{G})$ will simply equal 1. Sometimes, however, it is convenient to choose the conventional cell as being simple cubic and regarding the BCC and FCC lattices as SC lattices with two or four atom bases, respectively. In that case some of the SC diffraction spots will be missing. Thus, for the BCC lattice, let $\mathbf{s}_1 = \mathbf{0}$ and $\mathbf{s}_2 = (a/2)(\hat{i} + \hat{j} + \hat{k})$. For $\mathbf{G} = (2\pi/a)(n_1\hat{i} + n_2\hat{j} + n_3\hat{k})$ it follows that

$$S(\mathbf{G}) = 1 + e^{i\pi(n_1+n_2+n_3)}, \quad (3.47)$$

which is either 2 or 0, depending on whether $n_1 + n_2 + n_3$ is even or odd, respectively. Similarly, for the FCC lattice with $\mathbf{s}_1 = \mathbf{0}$, $\mathbf{s}_2 = (a/2)(\hat{j} + \hat{k})$, $\mathbf{s}_3 = (a/2)(\hat{k} + \hat{i})$, and $\mathbf{s}_4 = (a/2)(\hat{i} + \hat{j})$,

$$S(\mathbf{q}) = 1 + e^{i\pi(n_2+n_3)} + e^{i\pi(n_1+n_3)} + e^{i\pi(n_1+n_2)}, \quad (3.48)$$

which is either 4 (if the n_i are all even or all odd) or 0.

As another example of the calculation of the geometric structure factor, consider Si. The crystal is of the diamond crystal structure: an FCC lattice with a two-atom basis. The Si atoms in the basis are at $\mathbf{s}_1 = \mathbf{0}$ and at $\mathbf{s}_2 = a(\hat{i} + \hat{j} + \hat{k})/4$. The geometric structure factor is

$$S(\mathbf{q}) = \sum_j e^{i\mathbf{q}\cdot\mathbf{s}_j} = 1 + e^{i(a/4)(q_x+q_y+q_z)}. \quad (3.49)$$

Setting $\mathbf{q} = \mathbf{G} = j_1\mathbf{g}_1 + j_2\mathbf{g}_2 + j_3\mathbf{g}_3$ and using the primitive reciprocal lattice vectors for the FCC lattice gives

$$q_x = \frac{2\pi}{a}(-j_1 + j_2 + j_3), \quad q_y = \frac{2\pi}{a}(j_1 - j_2 + j_3), \quad q_z = \frac{2\pi}{a}(j_1 + j_2 - j_3). \quad (3.50)$$

Thus

$$\begin{aligned} [S(\mathbf{q})]_{\text{diamond}} &= [S(\mathbf{q})]_{\text{FCC}} [1 + e^{i(\pi/2)(j_1+j_2+j_3)}] \\ &= \begin{cases} 2 & \text{if } j_1 + j_2 + j_3 \pmod{4} = 0 \\ 1 + i & \text{if } j_1 + j_2 + j_3 \pmod{4} = 1 \\ 0 & \text{if } j_1 + j_2 + j_3 \pmod{4} = 2 \\ 1 - i & \text{if } j_1 + j_2 + j_3 \pmod{4} = 3. \end{cases} \end{aligned} \quad (3.51)$$

The notation " $J \pmod{n}$ " means "take J modulus n ". For positive J one continues to subtract n from J until there is a positive remainder smaller than n . For negative J one adds as many n 's as are necessary to make the result positive.

It is worthwhile comparing the results for the monatomic FCC crystal structure with the result for the diamond crystal structure. For FCC crystal structures all the nonvanishing spots have the same intensity. For diamond the spots have intensities 4, 2, 0, and 2.

3.4 Bragg and von Laue Descriptions of Diffraction

There are two equivalent ways of describing how a diffraction pattern is produced, due to Bragg and von Laue, respectively. The Bragg description is based on a wave description of the probe beam and involves constructive interference of the waves. The von Laue picture is based on a particle description of the beam and is closely related to the conservation laws for energy and momentum.

Figure 3.6 illustrates both viewpoints. Beam 1 with wave vector \mathbf{k} is reflected into beam 1' with wave vector \mathbf{k}' from lattice plane p_1 . Similarly, beam 2, which is parallel to 1, diffracts from lattice plane p_2 into beam 2', which is parallel to 1'. The lattice planes are a distance d apart. The angles between the beams and the plane are θ . Note that the full scattering angle is given by $\phi = 2\theta$. Also note that $k' = k$ for elastic scattering. The path difference between the waves scattered from the two adjacent lattice planes is seen to be $2d \sin \theta$. The Bragg condition for constructive interference is that the path difference is an integer number of wavelengths

$$2d \sin \theta = n\lambda = n \frac{2\pi}{k}, \quad (3.52)$$

where n is an integer ($n = 1$ is the first-order diffraction, $n = 2$ the second order, etc.). This implies that

$$2k \sin \theta = nG_1 = G, \quad (3.53)$$

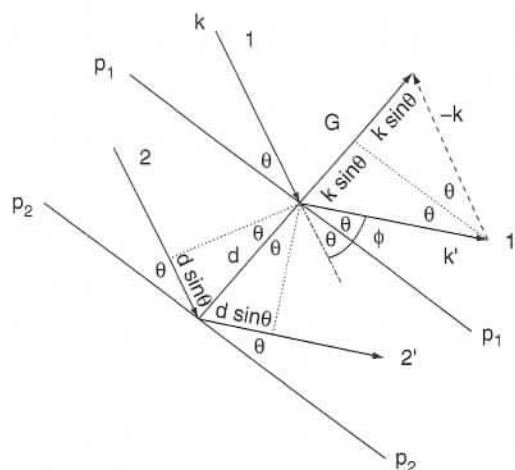


Figure 3.6. Diffraction from two lattice planes.

where $G_1 = 2\pi/d$ is an irreducible reciprocal lattice vector and G is a general reciprocal lattice vector.

It is important to note that the Bragg condition is related only to the lattice and provides no information about the basis atoms or the intensities of the diffraction maxima. Such information is provided by the structure factor of the basis and depends on the atomic form factors.

Von Laue argued that when particles scatter from a periodic structure, momentum will be conserved. Momentum may be transferred to or from the solid in units of $\hbar\mathbf{G}$ and the lattice recoils. However, since the lattice is so massive, the recoil carries with it very little energy. Thus

$$\mathbf{q} = \mathbf{k}' - \mathbf{k} = \mathbf{G}, \quad (3.54)$$

consistent with the Kronecker delta appearing in Eq. (3.40). This is illustrated graphically by the upper right-hand pair of triangles in Fig. 3.6. It is seen explicitly that $G = 2k \sin \theta$, in agreement with the Bragg result.

3.5 Polycrystalline Solids or Powders

Next consider a homogeneous material consisting of a set of randomly oriented and randomly spaced crystallites of finite size, such as is shown in Fig. 3.7 or Fig. 4.1b and c. The notation used to locate a given atom now needs to be enlarged. In analogy with Eq. (3.33), one has

$$\mathbf{A}_j(\mathbf{R}, \mathbf{U}) = \mathbf{U} + \mathbf{R}_U + \mathbf{S}_{U_j}. \quad (3.55)$$

Here \mathbf{U} locates a particular crystallite. Since the orientations of the lattices of the crystallites differ from each other, the lattice vectors \mathbf{R}_U are labeled by the vector \mathbf{U} . Similarly, vectors \mathbf{S}_{U_j} locating particular atoms within the unit cell now depend on the orientation of the crystallite and are also labeled by \mathbf{U} .

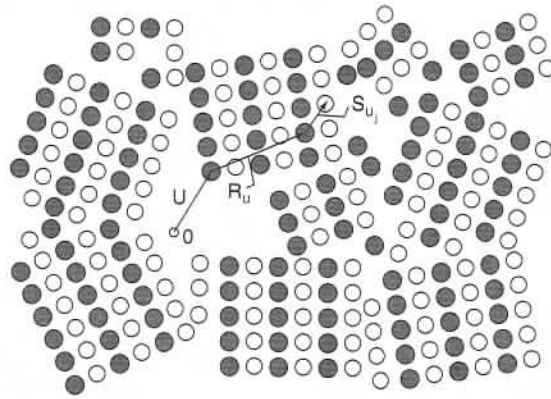


Figure 3.7. Polycrystalline solid.

The scattering intensity is given by

$$I(\mathbf{q}) \sim \left| \sum_{\mathbf{U}} \sum_{\mathbf{R}_U} \sum_{\mathbf{S}_{U_j}} f_j(\mathbf{q}) \exp[i\mathbf{q} \cdot (\mathbf{U} + \mathbf{R}_U + \mathbf{S}_{U_j})] \right|^2 \tag{3.56}$$

Note that the atomic form factor depends only on the type of atom at position \mathbf{S}_j .

The \mathbf{R}_U sum may be carried out first. There is a complication arising from the fact that each crystallite has a finite size. To analyze the situation, start with a one-dimensional "crystallite" with $2J + 1$ cells, where the lattice vectors are of the form $R_n = na$, and $n = -J, -J + 1, \dots, +J$. For such an object,

$$\begin{aligned} \sum_{n=-J}^J \exp(iqna) &= \exp(-iqJa) + \dots + \exp(iqJa) \\ &= \frac{\sin[(J + \frac{1}{2})qa]}{\sin(qa/2)}. \end{aligned} \tag{3.57}$$

The square of this function is shown in Fig. 3.8 for several values of J . It has a strong peak at $q = 0$ of size $2J + 1$ and then becomes smaller as qa increases. There are an infinite number of maxima and minima. The first time the function hits zero is at $qa = \pi/(J + 1/2)$. Thus a measure of the width Δq of the central peak gives the crystallite size, through the relation $Ja = 2\pi/\Delta q$. In the limit of large J this function narrows to a delta function, in agreement with the previously obtained result for the single crystal.

For a three-dimensional crystallite in the shape of a parallelepiped, this result may be generalized. Writing $\mathbf{R} = n_1\mathbf{u}_1 + n_2\mathbf{u}_2 + n_3\mathbf{u}_3$ and assuming that the indices range from $-J_i$ to J_i ($i = 1,2,3$), respectively, one obtains

$$\sum_{\mathbf{R}} \exp(i\mathbf{q} \cdot \mathbf{R}) = \prod_{i=1}^3 \frac{\sin[(J_i + \frac{1}{2})\mathbf{q} \cdot \mathbf{u}_i]}{\sin(\mathbf{q} \cdot \mathbf{u}_i/2)}. \tag{3.58}$$

Thus each diffraction peak is spread out, with the smaller crystallites producing the larger angular spread.

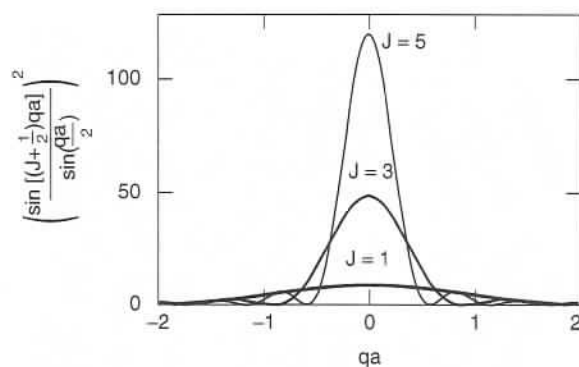


Figure 3.8. Square of the sum in Eq. (3.57) as a function of qa for three values of J : $J = 1$, 3, and 5.

Suppose that crystallites are sufficiently large that the sums may be represented as Kronecker deltas. Then

$$\sum_{\mathbf{R}_U} \exp(i\mathbf{q} \cdot \mathbf{R}_U) = N_c \sum_{\mathbf{G}_U} \delta_{\mathbf{q}, \mathbf{G}_U}, \quad (3.59)$$

where N_c is the number of atoms in the crystallite \mathbf{U} . Note that the reciprocal lattice vectors \mathbf{G}_U are referred to the orientation of the crystallite at \mathbf{U} . Thus one has (using a slightly abbreviated notation)

$$I = N_c^2 \sum_U \sum_{U'} \sum_s \sum_{s'} f_s(\mathbf{q}) f_{s'}^*(\mathbf{q}) \exp[i\mathbf{q} \cdot (\mathbf{U} - \mathbf{U}' + \mathbf{s} - \mathbf{s}')] \sum_{\mathbf{G}_U} \delta_{\mathbf{G}_U, \mathbf{q}}. \quad (3.60)$$

For simplicity's sake, the crystallites are all assumed to have the same size. Otherwise, N_c should be interpreted as an average number of atoms per crystallite. The locations of the crystallites are to a large extent random, although they do not overlap with each other. The sum over U' may be decomposed into two sums, one with $U' = U$ and the other with $U' \neq U$. It will be assumed that there is sufficient phase cancellation in the latter sum to replace it by zero. Then, using Eq. (3.35),

$$\begin{aligned} I &= N_c^2 \sum_U \sum_s \sum_{s'} f_s(\mathbf{q}) f_{s'}^*(\mathbf{q}) \exp[i\mathbf{q} \cdot (\mathbf{s} - \mathbf{s}')] \sum_{\mathbf{G}_U} \delta_{\mathbf{G}_U, \mathbf{q}} \\ &= N_c^2 \sum_U |\Phi(\mathbf{q})|^2 \sum_{\mathbf{G}_U} \delta_{\mathbf{G}_U, \mathbf{q}}. \end{aligned} \quad (3.61)$$

This shows that the total diffraction intensity is given by an incoherent sum of contributions stemming from the individual crystallites. These crystallites can often be expected to have random orientations. Correspondingly, the reciprocal lattices will also have random orientations in space.

The situation may be represented diagrammatically using the Ewald sphere. Energy conservation implies that $k = k'$, so both the initial and final photon wave vectors may be drawn as radii of a common sphere. This is illustrated in Fig. 3.9. In this figure ϕ denotes the scattering angle. Note that it is convenient to draw the vector \mathbf{k} twice. The

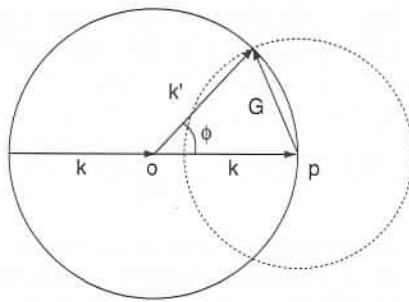


Figure 3.9. Ewald sphere depiction of the diffraction from a polycrystalline solid. The left sphere denotes energy conservation. The right sphere results from averaging over all crystallite orientations.

intersection of the two spheres satisfies the von Laue condition and produces a circle. The scattered x-rays lie on the surfaces of a set of cones whose vertex half-angles are given by

$$(3.59) \quad G = 2k \sin \frac{\phi}{2} = 2k \sin \theta. \quad (3.62)$$

The result is that the diffraction pattern consists of a set of rings, each produced by a different value of G . The sharpness of these rings is determined by the crystallite size, N_c . In the limit of large N_c the rings will be sharp.

If the temperature of the crystal is raised and the lattice vibrates more vigorously, two things happen. First, the rings still remain sharp, but their intensity diminishes. Second, a thermal diffuse background appears with x-rays being scattered to all angles. A discussion of this effect, the Debye-Waller effect, is given in Chapter W22.

3.6 Elastic Scattering from an Amorphous Solid

In an amorphous solid there is no long-range order, although there may be varying amounts of short-range order, as described in Chapter 4. It differs from the polycrystalline material, where there is "long"-range order within each crystallite. The factorization of the problem into lattice contributions and basis contributions is no longer possible, and this creates complications.

Suppose that there are N_A atoms located at sites \mathbf{r}_n . The scattering intensity for momentum transfer $\hbar\mathbf{q}$ is

$$(3.61) \quad I(\mathbf{q}) \sim \left| \sum_{n=1}^{N_A} f_n(\mathbf{q}) e^{i\mathbf{q} \cdot \mathbf{r}_n} \right|^2, \quad (3.63)$$

where $f_n(\mathbf{q})$ is the atomic form factor for the n th atom. Writing this as a double sum and separating the diagonal terms yields

$$(3.64) \quad I(\mathbf{q}) \sim \sum_n |f_n(\mathbf{q})|^2 + \sum_{n,m} ' f_n(\mathbf{q}) f_m^*(\mathbf{q}) e^{i\mathbf{q} \cdot (\mathbf{r}_n - \mathbf{r}_m)},$$

where the prime implies that $m \neq n$. First consider a monatomic solid for which there is only one atomic form factor $f(\mathbf{q})$ for all n . Introduce the pair or radial distribution function $g(\mathbf{r})$ defined by

$$\rho(\mathbf{r}) = \rho_0(g(\mathbf{r}) - 1) \equiv \frac{1}{N_A} \sum_{n,m}' \delta(\mathbf{r} - (\mathbf{r}_n - \mathbf{r}_m)). \quad (3.65)$$

The quantity $\rho(\mathbf{r})$ is the concentration of atoms at a distance r from a central atom, and ρ_0 is the average atomic density. It is assumed that a macroscopic piece of amorphous material has no preferred direction, so $g(\mathbf{r}) = g(r)$ will be isotropic. The expression for I may be rewritten as

$$\begin{aligned} I(\mathbf{q}) &= |f(\mathbf{q})|^2 \left[N_A + \sum_{n,m}' e^{i\mathbf{q} \cdot (\mathbf{r}_n - \mathbf{r}_m)} \right] \\ &= N_A |f(\mathbf{q})|^2 \left[1 + \int d\mathbf{r} \frac{1}{N_A} \sum_{n,m}' \delta(\mathbf{r} - (\mathbf{r}_n - \mathbf{r}_m)) e^{i\mathbf{q} \cdot \mathbf{r}} \right] \\ &= N_A |f(\mathbf{q})|^2 \left[1 + \rho_0 \int d\mathbf{r} (g(r) - 1) e^{i\mathbf{q} \cdot \mathbf{r}} \right]. \end{aligned} \quad (3.66)$$

The inverse Fourier transform gives the pair distribution function in terms of the intensity:

$$\begin{aligned} g(r) &= 1 + \frac{1}{\rho_0} \int \frac{d\mathbf{q}}{(2\pi)^3} \left[\frac{I(\mathbf{q})}{N_A |f(\mathbf{q})|^2} - 1 \right] e^{-i\mathbf{q} \cdot \mathbf{r}} \\ &= 1 + \frac{1}{2\pi^2 r \rho_0} \int_0^\infty \left[\frac{I(q)}{N_A |f(q)|^2} - 1 \right] \sin(qr) dq. \end{aligned} \quad (3.67)$$

The pair distribution function $g(r)$ gives the relative probability of finding an atom at a distance r from a given atom and can be calculated from the measured structure factor $I/N|f|^2$. The probability for finding the atom closer than an atomic radius is extremely small because of the interatomic repulsion. For large r , in the absence of long-range order, $g(r)$ will approach a constant. Peaks in $g(r)$ versus r indicate popular interatomic distances. The quantity $G(r) = 4\pi\rho_0 r [g(r) - 1]$ is called the *reduced radial distribution function*. The case $g(r) = 1$ corresponds to a continuum rather than a periodic array of discrete atoms. An example of $G(r)$ for the metallic glass $\text{Ni}_{0.76}\text{P}_{0.24}$ is shown in Fig. 4.11.

A brief discussion of the generalization of WS cells for amorphous solids is given in Section W3.1.

REFERENCES

- Azaroff, L. V., *Elements of X-ray Crystallography*, McGraw-Hill, New York, 1968.
 Azaroff, L. V., and M. J. Buerger, *The Powder Method in X-ray Crystallography*, McGraw-Hill, New York, 1968.
 Cullity, B. D., *Elements of X-ray Diffraction*, 2nd ed., Addison-Wesley, Reading, Mass., 1978.

Henry, N. F. M., and K. Lonsdale, eds., *International Tables for X-ray Crystallography*, International Union of Crystallography, Birmingham, England, 1969.

Klein, C., and C. X. Hurlbut, Jr., *Manual of Mineralogy*, Wiley, New York, 1985.

Klug, H. P., and L. E. Alexander, *X-ray Diffraction Procedures for Polycrystalline and Amorphous Materials*, Wiley, New York, 1954.

Schwartz, L. H., and J. B. Cohen, *Diffraction from Materials, 2nd ed.*, Springer Verlag, New York, 1987.

PROBLEMS

3.1 Prove that $\sum_{\mathbf{R}} \exp(i\mathbf{q} \cdot \mathbf{R}) = 0$, where $\{\mathbf{R}\}$ is a set of Bravais lattice vectors and $\mathbf{q} (\neq \mathbf{0})$ lies within the primitive unit cell of the reciprocal lattice. Also prove the orthogonality identity appearing in Eq. (3.12):

$$\int_{WS} e^{i(\mathbf{G}-\mathbf{G}') \cdot \mathbf{r}} d\mathbf{r} = V_{WS} \delta_{\mathbf{G}, \mathbf{G}'}$$

3.2 Find the Fourier coefficients V_n for the periodic functions $V(x) = A \sin(2\pi x/a)$ and $V(x) = B \cos(2\pi x/a)$.

3.3 Prove that the plane defined by the equation $\mathbf{G} \cdot \mathbf{r} = A$ lies a distance $d = A/G$ from the origin and that the normal to the plane is parallel to $\hat{\mathbf{G}}$.

3.4 Use the results of Problem 3.3 to generate formulas for the bounding planes of the first Brillouin zones for the FCC, BCC, and HCP crystal structures.

3.5 Determine the structure factor for the basis, $\Phi(\mathbf{q})$, defined in Eq. (3.35), for the cubic ZnS, CsCl, and NaCl crystal structures.

3.6 Draw the x-ray ring patterns produced by diffractions from powders for the SC, FCC, BCC, and diamond crystal structures.

3.7 Given an amorphous solid in which each atom has an electron density described by $n(r) = A \exp(-2r/a)$ and the pair distribution function is the unit step function $g(r) = \Theta(r - b)$, find the expected scattering intensity.

3.8 Sketch the Wigner-Seitz cell for the HCP crystal structure.

3.9 Find the distances from the center of the Wigner-Seitz cells for the BCC, FCC, and HCP crystal structures to the centers of the faces of the cells.

3.10 The primitive translation vectors of the hexagonal lattice can be written as

$$\mathbf{u}_1 = \hat{i} \frac{a\sqrt{3}}{2} + \hat{j} \frac{a}{2}, \quad \mathbf{u}_2 = -\hat{i} \frac{a\sqrt{3}}{2} + \hat{j} \frac{a}{2}, \quad \mathbf{u}_3 = c\hat{k}$$

(a) Show that the fundamental translation vectors of the reciprocal lattice are given by

$$\mathbf{g}_1 = \hat{i} \frac{2\pi}{a\sqrt{3}} + \hat{j} \frac{2\pi}{a}, \quad \mathbf{g}_2 = -\hat{i} \frac{2\pi}{a\sqrt{3}} + \hat{j} \frac{2\pi}{a}, \quad \mathbf{g}_3 = \frac{2\pi}{c} \hat{k}$$

(b) Describe and sketch the first Brillouin zone of the hexagonal lattice.

- (c) Prove that the perpendicular distance $d(hkl)$ between adjacent parallel planes in the hexagonal lattice is

$$d(hkl) = \frac{1}{\sqrt{\frac{4(h^2 + hk + k^2)}{3a^2} + \frac{l^2}{c^2}}}$$

[Hint: Use $d(hkl) = 2\pi/|G(hkl)|$.]

- 3.11 Find the shortest $\mathbf{G}(hkl)$ for (a) the BCC crystal structure, and (b) the FCC crystal structure.

Note: An additional problem is given in Chapter W3.